Bull. Chem. Soc. Ethiop. **2021**, 35(3), 669-675.
DOI: https://dx.doi.org/10.4314/bcse.v35i3.17
© 2021 Chemical Society of Ethiopia and The Authors
ISSN 1011-3924
Printed in Ethiopia
Online ISSN 1726-801X

SHORT COMMUNICATION

MICRORODS SYNTHESIZED OF MoO_3 WITH CORN STRAW AS BIOLOGICAL TEMPLATES AND ITS ELECTROCHEMICAL PERFORMANCE IN AQUEOUS ALUMINUM-ION BATTERY

Jianzhi Sun[1*], Yan Dong[1*], Xinfang Wang[1], Jiatao Cao[1], Man Gong[1] and Chunhui Li[2]

[1]College of Chemistry and Chemical Engineering, Dezhou University, Shandong Dezhou, 253023, China
[2]Experiment Management Centre, Dezhou University, Shandong Dezhou, 253023, China

(Received March 1, 2020; Revised January 19, 2022; Accepted January 20, 2022)

ABSTRACT. In this paper, MoO_3 microrods were prepared using corn straw as biological template via roasting process The components and crystal characterization of the material were investigated via X-ray diffraction (XRD), scanning electron microscopy (SEM), and the electrochemistry property and mechanism were studied. The results showed that the MoO_3 material synthesized by template method is orthorhombic structures. The MoO_3 particles were submicron and micron rods with uniform distribution and a smooth surface. MoO_3 microrods had an average diameter that ranged from 1 to 2 μm. The result indicated that the MoO_3 as the new negative of aluminum battery delivers a higher discharge capacity of 190 $mA \cdot h \cdot g^{-1}$ at a scanning rate of 1 $mV \cdot s^{-1}$, which showing good capacity and cycling performance.

KEY WORDS: Biological template, Corn straw, Aqueous aluminum-ion battery, MoO_3

INTRODUCTION

With growing concern about the environment, climate change and a sustainable energy supply, studies have been focused on the development of green energy storage systems with high volumetric energy density, low price and improved safety. In order to solve discontinuous and instable problems of renewable electricity (such as solar arrays and wind farms), energy storage systems can be used. The advanced new batteries are needed to have not only high energy density, but also good safety and affordable electric storage systems that enable better use of the intermittent renewable energy sources [1-3]. Because of superior performance in various electrochemical aspects, Li-ion batteries are often viewed as an energy storage device. However, limited resource and high price of lithium salts restrict its application in this area.

Orthorhombic molybdenum trioxide (α-MoO_3) has been extensively investigated as a key material for fundamental research and technological applications in photocatalyst, solar cells and electrochemical storage. The most important structural characteristic of α-MoO_3 is its structural anisotropy, which can be considered as a layered structure parallel to (010). Each layer is composed of two sub-layers, each of which is formed by corner-sharing octahedral along [001] and [100]; the two sub-layers stack together by sharing the edges of the octahedra along [001]. An alternate stack of these layered sheets along [010] would lead to the formation of α-MoO_3, where a van der Waals interaction would be the major binding force between the piled sheets [4, 5]. However, there are few literatures about the report of its electrochemical performance in aqueous rechargeable aluminum-ion battery.

Biological templates have attracted considerable attention for the syntheses of inorganic materials in the recent several years [6], because they are generally performed under mild

*Corresponding author. E-mail: jianzhisun@163.com; sddzdy@163.com
This work is licensed under the Creative Commons Attribution 4.0 International License

condition, it is energy-conserving, green, and has little requirement for equipment. Moreover, most natural templates and building blocks can be harvested in large amounts at low costs, thus biomorphic assembly is cheap compared with conventional assembly methods to form nanostructures.

Corn is one of major crops cultivated in China. There are about 0.2 billion tons of corn stalk produced annually. As agricultural waste in the world, the corn stalk has been widely used because of its many advantages, including easy preparation and low cost economical [7].

Aqueous aluminum ion batteries have become a hot spot for research because of the good safety performance, simple production and non-toxic electrolyte, high ionic conductivity and environmental friendliness [8-11]. Molybdenum trioxide (MoO_3), as a potential negative electrode material has a lot of advantages, such as high electrochemical activity, low cost, and environmentally friendly nature [12, 13]. However, there are few literatures about the report of its electrochemical performance in aqueous rechargeable aluminum-ion battery. In this study, MoO_3 was prepared by the solid-phase method and hydrothermal method and its electrochemical behavior in 1.0 mol·L^{-1} $AlCl_3$ aqueous solution is discussed.

EXPERIMENTAL

Sample preparation. The MoO_3 was synthesized via solid-phase method and biological templates method. MoO_3(I) was prepared by solid state reaction. Ammonium molybdate ($H_{24}Mo_7N_6O_{24}·4H_2O$) was placed in a tubular furnace with the heating temperature from 20 to 350 °C at 5 °C/min in air and incubated at 350 °C for a further two hours.

The MoO_3(II) was synthesized by biological templates method. The corn stalk was washed thoroughly with water to remove the adhering soil and dust. Then, in order to improve adsorption ability of corn straw, they were cut and immersed in 5% ammonia solution at room temperature for 8 h to eliminate hemicelluloses, lignin and some other components. The corn stalk was washed to the neutral with distilled water and further dried in an oven at 60 °C until they were completely dehydrated before are used. Then the dehydrated corn stalk was simply dipped into 0.5 mol/L ammonium molybdate solution for 24 h. The sample was washed with distilled three times and dried in an oven at 60 °C. After repeating this procedure for several cycles, the specimens were pyrolyzed at 550 °C for 4 h in air atmosphere with slow heating rate of 1 °C/min up to 300 °C and a higher rate of 2 °C/min up to 550 °C. After naturally cooling to room temperature, a white product, MoO_3 was obtained.

Characterization. X-ray diffraction(XRD) was performed on a Bruker D8A25 X-Ray diffractometer, the X-ray beam was nickel-filtered Cu Kα (λ = 0.15406 nm) radiation operated at 40 kV and 30 mA; and the data were collected from 10 ° to 80 °(2θ) at a scanning rate of 5 °/min.

The morphology of the samples was observed by JEOL JSM-5600LV SEM. EDX analysis was observed by Oxford Instruments.

Electrochemical measurements. Electrochemical characterization of the MoO_3 sample was carried out using three-electrode cells, in which a Graphite rod and an Ag-AgCl electrode served as a counter and reference electrodes. The working electrodes were prepared by pressing a 1 cm^2 thin film onto graphite paper. The sample electrode pellet was prepared by pressing the 8:1:1 (in wt.) mixture of active materials, acetylene black and polyvinylidene fluoride (PVDF). The electrolyte was 1.0 mol/L $AlCl_3$ solution purged with nitrogen before use. Cyclic voltammetry (CV) measurements were performed on a Ivium C16430 Electrochemical Analyst multichannel workstation manufactured by the Ivium Technologies with the cutoff voltage of -0.6/0.2 V at room temperature.

RESULTS AND DISCUSSION

XRD measurement was first used to study the phase and lattice modification of the biotemplated MoO_3(II) and the MoO_3(I) sample prepared by solid state reaction. The corresponding X-ray power diffraction patterns obtained at room temperature are presented in Figure 1. The diffraction peaks of the XRD pattern for both samples can be readily indexed to be orthorhombic structures with space group Pbnm (62) and the cell parameters: a = 0.3963 nm, b = 1.3856 nm, c = 0.36966 nm (International Centre for Diffraction Data (ICDD) No. 35-0609). The characteristic peaks at 2θ = 12.7°, 23.3°, 25.7°, 27.3°, 33.7°, 39.0° and 49.2° corresponded to the (020), (110), (040), (021), (111), (060) and (002) planes of MoO_3, respectively. No peaks of any other phases were detected, indicating the high purity of both of MoO_3 (I) and MoO_3 (II) samples.

For the biotemplated MoO_3 (II) microrods, the stronger intensities of (020), (110), and (060) peaks than those for the bulk MoO_3 (I) sample prepared by solid state reaction indicates the anisotropic growth of the nanostructure as well as the preferred orientation of the microrods on the substrate. Importantly, in comparison to the MoO_3 (I) , there is a shift of the (020) peak toward a lower diffraction angle for the biotemplated MoO_3 (II) microrods. This is direct evidence of an expanded *b*-plane interlayer distance, possibly due to the introduction of corn stalk bio-template [14, 15]. According to Bragg's equation, the b-plane interlayer distance of the biotemplated MoO_3 (II) microrods increased from 1.387 nm to 1.425 nm with decreasing 2θ from 12.7619 to 12.4228.

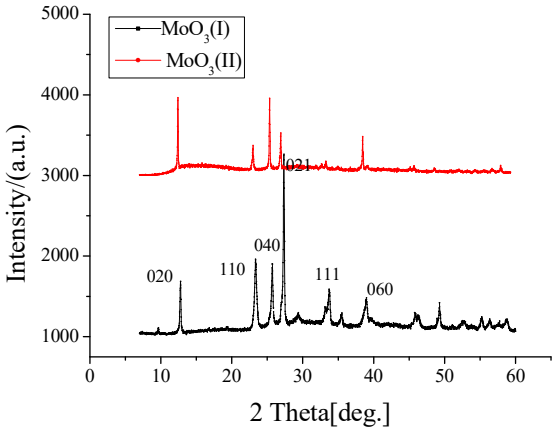

Figure 1. The XRD patterns of MoO_3 (I) and MoO_3 (II) samples.

The morphology and microstructure of the products were observed by using SEM. Figure 2 shows microstructure of the specimen. The results showed that the sample MoO_3 (I) was formed as a massive structure with different particles agglomerated together, and most of the particles are approximately 1–4 μm. The sample MoO_3 (II) showed a long segments with widths of 1–2 m and lengths of 3–10 μm, and a rectangle like cross section was clearly visible. The MoO_3 (II) can duplicate the biological structure of corn straw profect, having special structure, uniform morphology and good dispersion. The elemental compositions of the MoO_3 (II) were determined by energy dispersive X-ray spectroscopy (EDX). The result reflects the ratio of molybdenum to oxygen is about 1:3 in Figure 3.

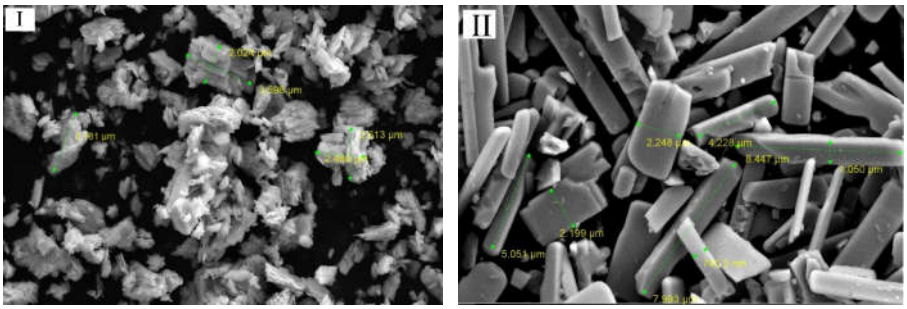

Figure 2. SEM images of MoO_3 (I) and MoO_3 (II) samples.

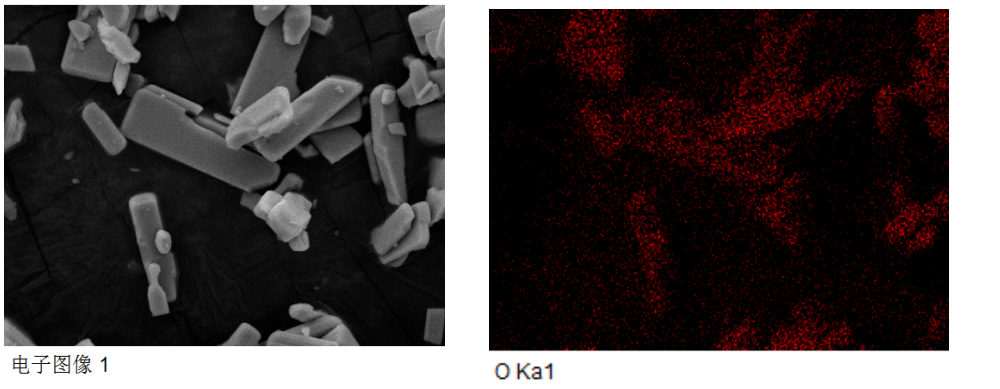

Figure 3. SEM-EDX images of the MoO_3 (II) sample.

Figures 4 and 5 show the CV of MoO_3 samples electrode in aqueous $AlCl_3$ electrolyte in the potential range of -0.6 to 0.2 V at a scan rate of 1 mV/s. As shown in Figure 4, the main CV feature appears as three pairs of symmetric redox peaks at 0.01/-0.14 V, -0.06/-0.19V, and -0.39/-0.53 V. These results of CV suggest that the redox peaks result from the Al^{3+} ions [16]. MoO_3 can

be used as the negative electrode material for aqueous aluminum ion batteries. Cyclic voltammetry tests showed that the MoO_3 (II) sample had a more obvious oxidation/reduction peak, the peak type was sharper and the peak current was higher. The discharge capacity of MoO_3 (I) and MoO_3 (II) samples were 74 $mAh \cdot g^{-1}$ and 190 $mAh \cdot g^{-1}$ after 5 cycles, respectively. Compared with MoO_3 (I), MoO_3 (II) clearly showed higher discharge capacities and better cyclic ability.

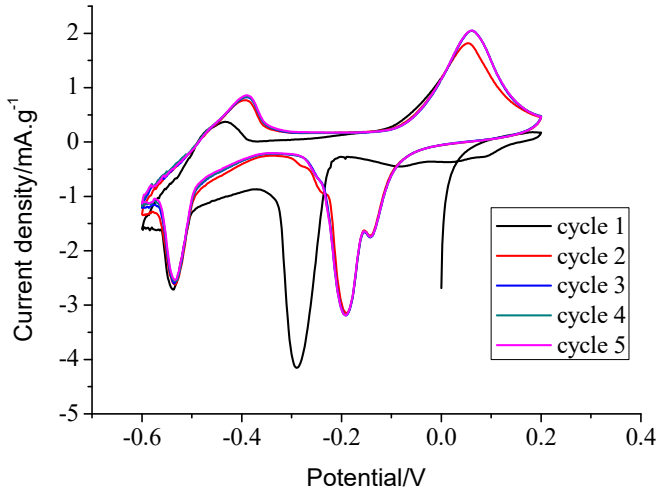

Figure 4. CV curves of measured MoO_3 (I) at a scan rate of 1 mV/s.

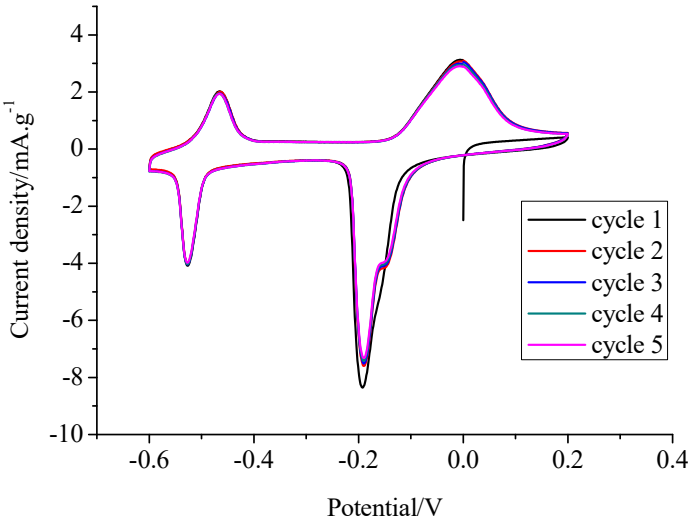

Figure 5. CV curves of measured MoO_3 (II) at a scan rate of 1 mV/s.

CONCLUSION

MoO_3 materials were prepared by using solid-phase method and biological template method exhibited distinct and reversible electrochemical intercalation behavior. Preliminary electrochemical data demonstrated that MoO_3 (II) showed a higher peak current, a larger discharge capacity and a better recyclability compared with MoO_3 (I). The discharge capacity of MoO_3 (II) is 190 $mAh \cdot g^{-1}$ in the 5th cycle at a current density of 1 mV/s. An optimization of both the material structure and the electrolyte compatibility is necessary to increase the specific capacity and cycle performance.

ACKNOWLEDGEMENTS

The authors acknowledge financial assistance from the Undergraduate University Teaching Reform Research Project of Shandong (M2018X015) and the Natural Science Foundation of Shandong (ZR2014JL011).

REFERENCES

1. Dominique L.; Tarascon J. M. Towards greener and more sustainable batteries for electrical energy storage. *Nature Chem.* **2015**, 7, 19-29.
2. Sun J.Z.; Dong Y.; Kong C.Y. Synthesis of $Na_2MnFe(CN)_6$ and its Application as Cathode Material for Aqueous Rechargeable Sodium-ion Battery. *J. New Mat. Electrochem. Syst.* **2016**, 19, 117-119.
3. Zhang H.Y.; Cao D.X.; Bai X. High rate performance of aqueous magnesium-ion batteries based on the δ-MnO_2@carbon molecular sieves composite as the cathode and nanowire VO_2 as the anode. *J. Power Source*s **2019**, 444, 227299-227305.
4. Mai L.Q.; Hu B.; Chen W.; Qi Y.Y.; Lao C.S.; Yang R.S.; Wang Z.L. Lithiated MoO_3 Nanobelts with Greatly Improved Performance for Lithium Batteries. *Adv. Mater.* **2007**, 19, 3712-3716.
5. Li T.Q.; Beidaghi M.J.; Xiao X.; Huang L.; Hu Z.M.; Sun W.M.; Chen X.; Gogotsi Y.; Zhou J. Ethanol reduced molybdenum trioxide for Li-ion capacitors. *Nano Energy* **2016**, 26, 100-107.
6. Liu C.; Wu F.; Su Q.Q.; Qian W.P. Template Preparation and Application in Biological Detection of Porous Noble Metal Nanostructures. *Prog. Chem.* **2019**, 8, 1396-1405.
7. Huang Y.T.; Ying Z.P.; Zheng J.X.; Zhuang S.G.; Liu L.; Feng W. Hierarchical porous ZnO nanomaterial synthesized with corn straw as biological templates and its photocatalytic performance. *Chem. J. Chin. Univ.* **2018**, 39, 2031-2038.
8. Liu S.; Hu J.J.; Yan N.F.; Pan G.L.; Li G.R.; Gao X.P. Aluminum storage behavior of anatase TiO_2 nanotube arrays in aqueous solution for aluminum ion batteries. *Energy Environ. Sci.* **2012**, 5, 9743-9746.
9. Reed L.D.; Menke E. The roles of V_2O_5 and stainless steel in rechargeable Al-ion batteries. *J. Electrochem. Soc.* **2013**, 160, A915-917.
10. González J.R.; Nacimiento F.; Cabello M.; Alcántara R.; Lavela P.; Tirado J.L. Reversible intercalation of aluminum into vanadium pentoxide xerogel for aqueous rechargeable batteries. *RSC Adv.* **2016**, 6, 62157-62164.
11. Nacimiento F.; Cabello M.; Alcántara R.; Lavela P.; Tirado J. L. NASICON-type $Na_3V_2(PO_4)_3$ as a new positive electrode material for rechargeable aluminum battery. *Electrochim. Acta*, **2018**, 260, 798-804.
12. Wang F.X.; Liu Z.C.; Wang X.W.; Yuan X.H.; Wu X.W.; Zhu Y.S.; Fu L.J.; Wu Y.P. A conductive polymer coated MoO_3 anode enables an Al-ion capacitor with high performance. *J. Mater. Chem. A*, **2016**, 4, 5115-5123.

13. Ramachandran R.; Xuan W.L.; Zhao C.H.; Leng X.H.; Sun D.Z.; Luo D.; Wang F. Enhanced electrochemical properties of cerium metal-organic framework based composite electrodes for high-performance supercapacitor application. *RSC Adv.* **2018**, 7, 3462 -3469.
14. Lahan H.; Das S. K. Al^{3+} ion intercalation in MoO_3 for aqueous aluminum-ion battery. *J Power Sources* **2019**, 413, 134–138.
15. Lahan H.; Das S. K. Graphene and diglyme assisted improved Al^{3+} ion storage in MoO_3 nanorod: Steps for high-performance aqueous aluminum-ion battery. *Ionics* **2019**, 25, 3493–3498.
16. Augustyn V.; Simon P.; Dunn B. Pseudocapacitive oxide materials for high-rate electrochemical energy storage. *Energy Environ. Sci.* **2014**, 7, 1597-1603.